CRITICAL TRACTIVE FORCE OF UNIFORM SANDS

by

Jimmy Frank Harp

A Dissertation Submitted to the Faculty of the

DEPARTMENT OF CIVIL ENGINEERING

In Partial Fulfillment of the Requirements

For the Degree of

DOCTOR OF PHILOSOPHY

In the Graduate College

THE UNIVERSITY OF ARIZONA

1963

THE UNIVERSITY OF ARIZONA

GRADUATE COLLEGE

I hereby recommend that this dissertation prepared under my direction by Jimmy Frank Harp

entitled CRITICAL TRACTIVE FORCE OF UNIFORM SANDS

be accepted as fulfilling the dissertation requirement of the degree of DOCTOR OF PHILOSOPHY

E. M. Laursen — May 27, 1963
Dissertation Director — Date

After inspection of the dissertation, the following members of the Final Examination Committee concur in its approval and recommend its acceptance:*

Morris W. Self	June 21, 1963
D. Tripp	June 25, 1963
J. F. Foster	June 28, 1963
H. P. Hansen	13 June 63
E. R. Parker	28 JUNE '63
A. Langer	June 27, 1963

*This approval and acceptance is contingent on the candidate's adequate performance and defense of this dissertation at the final oral examination. The inclusion of this sheet bound into the library copy of the dissertation is evidence of satisfactory performance at the final examination.

STATEMENT BY AUTHOR

This Dissertation has been submitted in partial fulfillment for an advanced degree at The University of Arizona and is deposited in the University Library to be made available to borrowers under rules of the Library.

Brief quotations from this Dissertation are allowable without special permission, provided that accurate acknowledgment of source is made. Requests for permission for extended quotation from or reproduction of this manuscript in whole or part may be granted by the head of the major department or the Dean of the Graduate College when in their judgment the proposed use of the material is in the interests of scholarship. In all other instances, however, permission must be obtained from the author.

Signed: Jimmy F. Harp

APPROVAL BY DISSERTATION DIRECTOR

This Dissertation has been approved on the date shown below:

E. M. Laursen

E. M. Laursen
Professor and Head of Civil Engineering

May 2, 1963
Date

ABSTRACT

Incipient motion of sand particles on channel boundaries is studied in order to provide an analytical solution for the conditions causing motion and to provide experimental data to verify these solutions. The results can be applied directly to various design aspects of the problem.

The experimental data substantiates the analytically derived equations in that experimental coefficients are determined from the data. Several basic assumptions are made to facilitate the mathematical formulations.

Shear stresses are measured directly by means of the Preston technique and the calibration curves of Laursen and Hwang. These small magnitude measurements are facilitated by the use of a very sensitive pressure cell in conjunction with an electronic indicator having high amplification. The heart of the analysis is unquestionably in the shear methods that have been developed only recently.

The results achieved in the analysis are compared with that of White and Shields, the classical investigators in the field.

ACKNOWLEDGMENT

The writer wishes to acknowledge and express his gratitude for the guidance and encouragement of his Dissertation Director, Dr. E. M. Laursen. The capable assistance afforded by Mr. Brooks Muterspaugh, technician of the Civil Engineering Laboratories, must also be mentioned. Finally, the writer must also acknowledge the constant confidence and encouragement of his wife, Zoe Ann.

TABLE OF CONTENTS

NOTATION

Symbol	Quantity
a	distance from channel bottom to zero datum, ft.
α	shape or volume factor
α_x	area factor (x refers to affected area)
A	area, sq. ft.
d	sand grain diameter, ft.
δ'	thickness of laminar boundary layer, ft.
D	distance from channel bottom to top of exposed grains, ft.
F_A	aerodynamic force, lb.
F_B	buoyant force, lb.
F_D	form-drag force, lb.
γ	specific weight, lb/cu. ft.
g	gravitational constant, ft/sec/sec.
h	distance from channel bottom to center of exposed particle, ft.
K	aerodynamic constant
k_s	roughness magnitude, ft.
ℓ	moment arm, ft.
μ	viscosity, lb-sec/sq. ft.
n	number of rows
N	normal force
ρ	mass density, slugs/cu. ft.
τ_c	critical tractive shear stress, lb/sq. ft.
τ_o	average shear stress, lb/sq. ft.
Q	flow rate, cu. ft./sec
v	velocity, ft/sec.

v_*	$\sqrt{\tau_o/\rho}$ the shear velocity, ft/sec.
V	average velocity, ft/sec.
V_c	average velocity at critical conditions, ft/sec.
~~V~~	volume of sand grain, cu. ft.
w	channel width, ft.
W	weight of sand grain, lb.
x, y, z	mathematical parameters

CHAPTER 1

INTRODUCTION TO THE PROBLEM

1.1 Introduction

The movement of water in canals and rivers has been the subject of scientific investigation and research for a long time. Eventually the rivers and streams in this country will carry to the oceans the greater percent of the weathered mountains. In the meantime man wishes to use the rivers and the water but problems often arise because of the sediments transported by the streams and those composing the boundaries of the streams.

In connection with the many sedimentation problems which arise in the field of hydraulics, the flow conditions causing incipient motion of the bed particles is often of interest. For example, if one is interested in designing an earth canal to transport clear water, the flow conditions must be such that no motion of the bed material occurs and that the channel will not scour. Other examples might be evaluating the scour below outlet works and stilling basins and the deposition in settling basins and reservoirs. These problems are characterized by a non-movement of the bed particles, and the design criterion should be such that the intensity of the boundary shear is equal to the critical intensity causing movement of the particular sediments.

A complete understanding of the boundary shear stresses which cause movement of the bed particles is essential to an understanding of the movements of sediments since it is only at intensities of shear

greater than the critical that sediment transport will occur.

In this era when man is preparing to depart to the moon and other celestial bodies it is provoking to realize that many of the phenomena of nature still cannot be explained. The words of Galileo are still appropriate, "I find less difficulty in the discovery of the planets, in spite of the great distance, than in the investigation of the flow of water which takes place right before my eyes."

1.2 The Problem Defined

The problem of this dissertation is to relate the average boundary shear to the incipient movement of sand particles on channel bottoms for both laminar and turbulent flow.

1.3 Method of Treatment

The problem is subject to both analytical and experimental analysis. The experimentation is performed in both the laminar and turbulent regimes of flow. In the laminar regime, the laboratory analysis entails approximating the forces on sediment particles in various possible positions among the other sediment particles. The turbulent flow regime analysis will consider the different intensities of turbulence in the flow conditions. In both cases, the solution can only be approximated and involves undetermined experimental coefficients. The experimental results allow an estimate of those constants and in essence verify the analytical analysis.

1.4 Literature Survey

A complete literature survey into the material pertinent to this problem would be an extensive work. For this reason, only the papers and articles which are representative of the history of the

problem will be reviewed. The studies of importance can be broadly classed into three divisions; surface-resistance, sediment traction, and velocity distribution. The following material is divided in this way.

Surface-Resistance

The measurement of local surface-resistance or wall shearing stress is a very difficult technique, except in a few simple cases where it can be deduced from a known pressure drop. The measurement of shearing forces on an isolated element would be a direct approach in obtaining the local-surface-resistance. Although this technique requires a most complicated instrumentation, at least three attempts have been made for flat surfaces. In 1929, Kempf (1)* measured the surface-resistance on the flat bottom of a ship in a towing basin. The results are the only existing direct surface-resistance measurements at high Reynolds numbers. In 1941, Schultz-Grunow (2) used a similar technique to measure the frictional forces on a wind-tunnel wall. More recently, in 1951, Dhawan (3) obtained further surface-resistance data on a flat plate at low Reynolds numbers. Unfortunately, this technique is very difficult for general use. In 1930, Fage and Falkner (4) used a calibrated half-pitot-tube in the laminar sublayer to correlate pressures with local surface-resistance. Because of the extremely small size of the tube, the sensitivity of the test probe, and other uncertainties, application of the method is difficult.

---

*Numbers in parentheses refer to REFERENCES.

Local surface-resistance can also be obtained indirectly from a velocity traverse together with the momentum equation. This method is both tedious and inaccurate since the local surface-resistance is the small difference between two large values. In 1950, Ludweig (5) developed the hot spot technique and obtained the local surface-resistance by measuring the heat-loss from a heated spot within the laminar sublayer of the flow medium. Great care must be taken with the insulation, however, since an unknown amount of heat is transferred to the wall. In 1954, Preston (6) utilized the simple technique of measuring the local surface-resistance by means of a pitot-tube resting on the boundary of a smooth surface. This method is based on the assumption of an inner law relating the local shear to the velocity distribution near the wall. Using the pressure drop in a pipe to calibrate the instrument, Preston obtained equations relating the intensity of shear to the pitot-tube reading for the case of the laminar sublayer enveloping the tube and for the case of the tube in the turbulent boundary layer on the smooth surface. His calibrations give an empirical relationship which is apparently quite reliable. In 1955, Hsu (7) extended the Preston shear method to cases where an adverse pressure gradient exists. He made an analysis using the one-seventh power velocity distribution in the derivation of his turbulent flow equation at moderate values of Reynolds numbers. In the laminar sublayer he used a linear velocity distribution. In 1962, Laursen and Hwang (8) extended the method even further to be applicable to rough boundaries. Both Hsu, and Laursen and Hwang have substantiated the Preston shear technique to the point

where it is not only feasible, but virtually opens the door to a whole new field of measurements that heretofore have not been possible.

Sediment Traction

Probably, the most widely quoted and best known analyses of incipient motion of sand grains on channel boundaries are those of White (9) in 1940 and Shields (10) in 1936. White sought to determine the factors which govern incipient motion by equating the moments which tend to move the grains to those which resist the motion. The resulting formula of White is thought to be valid only in a certain range of Reynolds numbers and flow conditions. Shields believed that it was not possible to express analytically the forces which act upon a typical particle. He avoided any such attempt at rationality by making certain gross assumptions and then substantiating and supplementing them experimentally. The resulting "Shields Diagram" is the accepted classical analysis in this field of endeavor.

In general, there has been some disagreement as to the nature of incipient motion. An example of this might be to compare Rubey's work in 1938 to that of Hjulstrom in 1939. Rubey (12) thought that for particles five mm in diameter and smaller, velocity rather than size was the dominating factor, where Hjulstrom (13) states that particle size rather than velocity is the pertinent criterion for incipient motion.

It is expedient at this point to mention some of the applications and ramifications of the boundary shear stress problem as it relates to the clear water canal. The Bureau of Reclamation has done

significant work on this subject recently. In 1951, Glover and Florey (14) showed that the tractive force, for smooth boundaries, is closely approximated by a simple expression. They emphasized that this expression, regardless of its simplicity, is very close to the true condition. In 1951, Olsen and Florey (15) worked out a mathematical procedure using finite differences as an analytical approach to the shear-distribution problem. The shear-distribution problem is of extreme importance because of the different magnitudes of shear stress that might exist in any one channel section and in different channel sections. Carter and Carlson (16), in 1953, worked out derivations for the ratio of the maximum to the average shear stress as a function of the channel shape. Lane (17), in 1955, and other earlier investigators, have studied the tractive force ratio of the shear stress on the sides to the average shear stress on the channel bottom as a function of the inclination of the sloping sides and the angle of repose of the material. This ratio is mainly of importance with respect to coarse noncohesive materials. More recently, in 1961, P. F. Enger (25) analyzed the tractive force fluctuations on open channel boundaries as measured from point velocity measurements.

In addition the Bureau of Reclamation has made a comprehensive study of the critical shear stress problem using data obtained from the San Luis Valley (18). As a result, values of the permissible tractive force in straight channels were conservatively estimated to be about 0.40 times the sediment diameter in inches, the diameter taken as that for which 25% of the sediment is larger, for coarse noncohesive sediments.

For sinous channels, the values should be lowered in order to obviate scour. Approximate percentages of reduction, suggested by Lane (19), are 10% for slightly sinous channels, 25% for moderately sinous channels, and 40% for very sinous channels. This reduction in permissible tractive force is really an expedient to compensate for an increased shear stress which is present in sinous channels.

Velocity Distributions

Because velocity distributions in pipes and channels are unquestionably related to the shear distribution problem, they must be considered critically since part of the derivation in this analysis depends upon their use.

Velocity distributions are generally expressed empirically because they are not theoretically derivable except in a few simple cases of laminar flow. An extensive discussion of this subject is found in many works, such as (20), (21), and (22), so only a survey is presented here.

The Karman-Prandtl velocity distribution equations, which are generally considered to be a satisfactory approximation for pipes and channels and are often used in other situations, can be expressed as follows:

$$v/v_* = A + B \log_{10} y/k_s \qquad (1.1)$$

and

$$v/v_* = A' + B' \log_{10} v_* y/k_s \qquad (1.2)$$

where Equation (1.1) is the rough form and the coefficients A and B, usually quoted from the classic experimental data of Nikuradse, are found to be 8.50 and 5.75 respectively. In Equation (1.2), the smooth

boundary form, the coefficients, from Nikuradse's data, are found to be 5.50 and 5.75 respectively, except in the transition region where A' and B' are a function of $\frac{v_* k_s}{\nu}$ or k_s/δ'. In the transition region, von Karman suggests values of A' and B' as -3.05 and 11.5, in Equation (1.2), as an acceptable approximation.

Logarithmic forms of velocity distributions can be derived analytically by assuming a shear stress distribution and equating it to one of the expressions which have been theorized for turbulent shear stress. Upon integrating and evaluating the constants, expressions similar to the above equations result. Prandtl and von Karman have both presented such expressions, and they agree generally with the experimental data of Nikuradse. The chief objection to the logarithmic equations arises in the fact that they do not satisfy the zero velocity condition at the boundary. Since the imperfection arises from the basic equation for turbulent shear stress, imperfect confirmation is to be expected. Even though a comprehensive equation for turbulent shear stress has not been developed, the Karman-Prandtl equations represent great progress toward that end. Although the adequacy of the logarithmic equations can be debated, especially near the boundary, and the indeterminancy of the zero datum presents difficulties, the equations are at least a good approximation.

For the case of laminar flow, the so-called inner-law expressed by

$$v/v_* = f\left(v_* y/\nu\right) \tag{1.3}$$

is often applied to the laminar sublayer in the linear form

$$v/v_* = v_* y/\nu \tag{1.4}$$

The linear approximation assumes a constant shear and is apparently very satisfactory. The most recent substantiation of the inner-law has been that of Ludweig and Tillman (23), in 1950, by means of the hot-spot technique mentioned earlier.

It must also be mentioned that the velocity distribution equations are sometimes expressed in the form of a power function instead of the unwieldy logarithmic relationships. In the analysis which follows, the empirical velocity distributions are used with full appreciation of the imperfections and the subsequent dangers involved.

CHAPTER 2

THEORETICAL ANALYSIS

Several investigators have attempted to obtain general analytical expressions relating critical tractive shear stress to flow parameters for wide ranges of Reynolds numbers. Until recently, however, no simple experimental method for determining these boundary shear stresses could be found so that analytical hypotheses could be verified. Now, with the new Preston shear technique, the problem can be approached with new confidence. The solutions presented here differ from any prior ones in that a complete analysis, accounting for all the forces, is made.

2.1 Critical Tractive Shear Stress Defined

Before the formal analysis is started, it is expedient to define just what is meant by critical tractive shear stress. We mean "the temporal spatial average intensity of shear when the more exposed particles are moved by the fluid forces at a maximum." Mathematically, it is expressed in the analysis which follows as

$$\tau_c = \tau_s + F_D/A_D \qquad (2.0)$$

when motion impends. This definition is the logical definition of critical shear stress in any complete analysis.

2.2 Statement of the Problem

With the fundamental notions of critical tractive shear stress now in mind, a basic analysis of incipient motion of uniform sands begins with a simple free-body diagram of a typical exposed particle, or grain.

The analysis is somewhat more complex because of the existence of the two regimes of flow and the transitional region.

In this analysis only three different cases of incipient motion are considered. They are (see Figure 1):

Case I. Laminar flow throughout.

Case II. Turbulent flow where the laminar boundary layer thickness δ' is greater than the grain heights D. i.e. $\delta' \gg D - a$.

Case III. Turbulent flow where the laminar boundary layer thickness δ' is less than the grain heights D. i.e. $\delta' \ll D - a$.

In Figure 1, the velocity distribution $v = f(y)$ is shown for clarification. It is measured from a zero datum which is unspecified and unknown. The distance "a" must be incorporated into the experimental coefficients. Some notions of this parameter do however place it within certain limits. The basic problem then reduces to the application of the equations of equilibrium, and subsequently deriving the expressions for form-drag and appropriately substituting into the equations of equilibrium.

2.3 Application of Equilibrium Equations

To begin, consider a typical exposed particle as shown in Figure 1, and draw the free-body diagram as in Figure 2. The forces acting on the particle are the usual expressions of basic mechanics.

Let us now apply the equations of equilibrium for impending motion of the particle shown in Figure 2.

This gives:

$$\Sigma F_x = 0 = \tau_s A_s + F_D - N \sin\theta \qquad (2.1)$$

$$\Sigma F_y = 0 = F_A + F_B - W + N\cos\theta \qquad (2.2)$$

$$\Sigma M_o = 0 = l_w(W - F_B) - l_s \tau_s A_s - l_D F_D - l_A F_A \qquad (2.3)$$

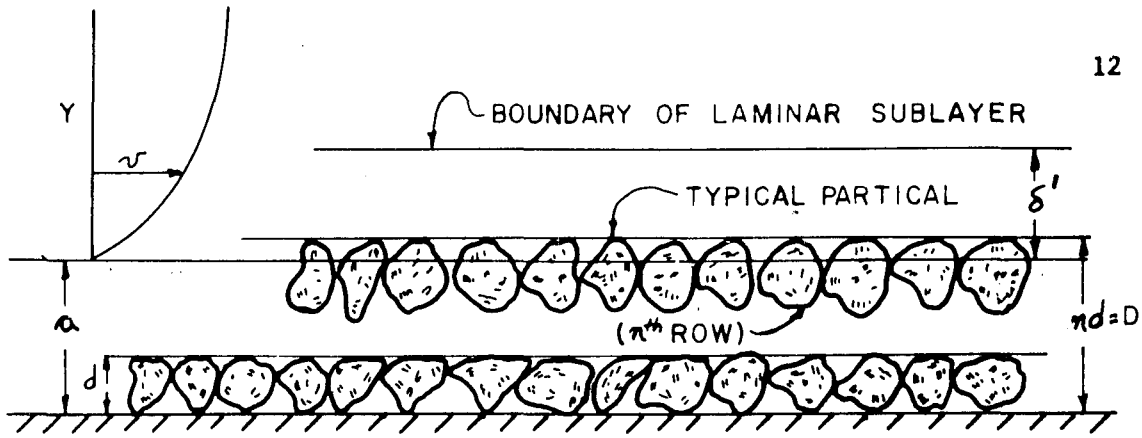

FIGURE 1

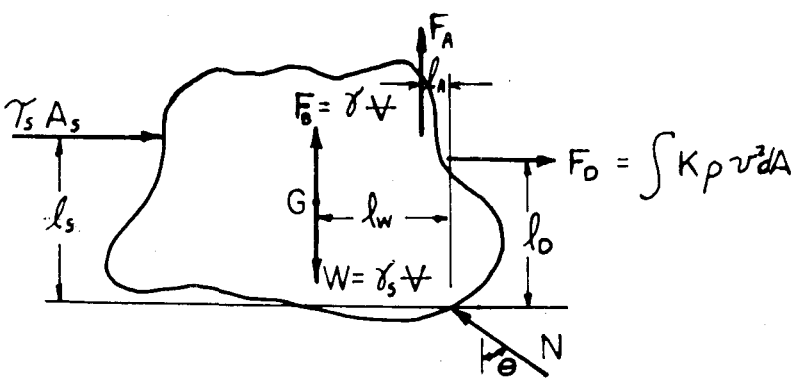

FIGURE 2

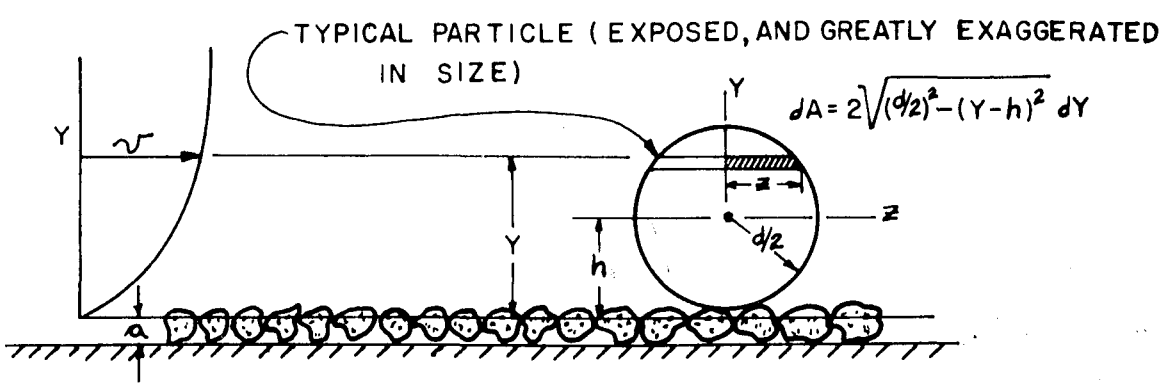

FIGURE 3

and eliminating the normal force N, and the aerodynamic force F_A, we have

$$\tau_s + C_2 F_D/d^2 = C_1 d(\gamma_s - \gamma) \qquad (2.4)$$

where $C_1 = \frac{l_w/l_a - 1}{l_s/l_a - \text{ctn}\theta}$ and $C_2 = \frac{l_D/l_a - \text{ctn}\theta}{(l_s/l_a - \text{ctn}\theta)\alpha_s}$

The constants C_1 and C_2, because of their nature, must be evaluated experimentally. Also we have made full use of the area and volume simplifications utilized by Anderson (24) such that $A_s = \alpha_s d^2$, $\forall = \alpha d^3$ etc. Equation (2.4) is valid for all three cases mentioned in article 2.2.

2.4 Derivation of Form-Drag Expressions

At this point, it is necessary to derive the expressions for the form-drag force F_D applicable to all three cases. This of course will have to be done in two parts, the first for the laminar regime, and the second for the turbulent regime. The general picture is shown in Figure 3. The following assumptions are made:

(1) The constant K is considered equal to the mean value for all values of y.
(2) Adjacent particles do not affect the velocity distribution in front of the particle.
(3) The grain is considered spherical in shape.
(4) For flow within the laminar sublayer, we assume that the well known relationship $v/v_* = v_* y/\nu$ holds.
(5) For turbulent flow over the particle, we assume that the logarithmic equation (1.1) expressed as $v/v_* = 2.50 \log_e 30 y/k_s$ is at least a good approximation.

Although the adequacy of these equations is debatable, especially near the boundary, and the indeterminancy of the zero datum presents problems, both of these expressions are used here for lack of more perfect ones.

Laminar flow throughout:

Take the basic drag equation $\int_A K\rho v^2 dA$ and using the expression mentioned in assumption 4, we obtain $F_D = 2K\rho \int_{h-d/2}^{h+d/2} (\tau_0 y/v\rho)^2 \sqrt{(d/2)^2-(y-h)^2}\, dy$ (2.5)

This equation is integrable with the aid of the following substitution:

$$y - h = d/2 \sin\theta \tag{2.6}$$

$$dy = d/2 \cos\theta\, d\theta \tag{2.7}$$

thus: $$F_D = \frac{2K\tau_0^2 (d/2)}{v^2\rho} \int_{-\pi/2}^{\pi/2} (h + d/2 \sin\theta)^2 \cos\theta \sqrt{(d/2)^2 - (d/2 \sin\theta)^2}\, d\theta \tag{2.8}$$

which reduces to

$$F_D = \frac{2K\tau_0^2 (d/2)^2}{v^2\rho} \int_{-\pi/2}^{\pi/2} (h^2 + h\, d \sin\theta + d^2/4 \sin^2\theta) \cos^2\theta\, d\theta \tag{2.9}$$

which is seen to be of the standard forms found in any table of integrals.

The final integrated form of Equation (2.9) reduces to

$$F_D = \frac{K\tau_0^2 \pi d^2}{v^2\rho\, 4} \left[h^2 + 0.0625 d^2\right] \tag{2.10}$$

and τ_D, the desired expression, becomes

$$\tau_D = F_D/A_D = \frac{K\tau_0^2}{v^2\rho} \left[h^2 + 0.0625 d^2\right] \tag{2.11}$$

Equation (2.11) holds for the case of laminar flow throughout and for the Case II where the laminar boundary layer is sufficiently thick.

Turbulent flow:

Now, to derive the form drag equation for turbulent flow, we simply substitute the equation mentioned in assumption 5 into the basic drag equation and get

$$F_D = 2K\rho v_*^2 (2.50)^2 \int_{h-d/2}^{h+d/2} \left(\log_e 30 y/k_s\right)^2 \sqrt{(d/2)^2 - (y-h)^2}\, dy \tag{2.12}$$

This equation is indeed formidable, but can be integrated as follows:

first make the substitutions $y - h = d/2 \sin\theta$

$A = 30h/k_s$

$B = 30(d/2k_s)$

$dy = d/2 \cos\theta\, d\theta$

to have $$F_D = \frac{2K\rho v_*^2 (2.50)^2 (d/2)^2}{2} \int_0^{2\pi} \left\{ \log_e (A + B\sin\theta) \right\}^2 \cos^2\theta \, d\theta \qquad (2.13)$$

which reduces to $$F_D = 1.562\,\tau_0 K d^2 \int_0^{2\pi} \left[\log_e (A + B\sin\theta) \right]^2 \cos^2\theta \, d\theta \qquad (2.14)$$

which is seen to be of the same form as that encountered by Laursen and Hwang (8). Hwang sought out a clever method, which is described in detail in that paper, and presents a solution to such an expression. According to Laursen and Hwang, Equation (2.14) integrates into:

$$F_D = 1.562\,\tau_0 K \pi d^2 \left\{ \left[\log_e 30h/k_s \right]^2 - \left(\log_e 30h/k_s \right) \left[0.25 (d/2h)^2 + 0.0625 (d/2h)^4 + 0.0260 (d/2h)^6 + \ldots \right] + \left[0.25 (d/2h)^2 + 0.1146 (d/2h)^4 + 0.0586 (d/2h)^6 + \ldots \right] \right\} \qquad (2.15)$$

Since τ_D is the desired result, we have $$\tau_D = C_4 \tau_0 \qquad (2.16)$$

where $C_4 = 6.248 K S$ and $$S = \left\{ \left[\log_e 30h/k_s \right]^2 - \left(\log_e 30h/k_s \right) \left(0.25 (d/2h)^2 + 0.0625 (d/2h)^4 + 0.0260 (d/2h)^6 + \ldots \right] + \left[0.25 (d/2h)^2 + 0.1146 (d/2h)^4 + 0.0586 (d/2h)^6 + \ldots \right] \right\}$$

2.5 Substituting the Form-Drag Equations Into Equation (2.4)

Having derived the expressions for form-drag, we are ready to substitute into the basic equation. Again considering laminar flow first and putting Equation (2.11) into Equation (2.4) we have

$$\tau_c = \tau_s + F_D/A_D = \left[C_1 d(\gamma_s - \gamma) - C_2 F_D/d^2 \right] + \tau_D$$

$$\tau_c = \left[C_1 d(\gamma_s - \gamma) \right] - \frac{C_2 K \tau_0^2 (h^2 + 0.0625 d^2)}{4\nu^2\rho} + \frac{K\tau_0^2}{\nu^2\rho} \left[h^2 + 0.0625 d^2 \right]$$

$$\tau_c = C_1 d(\gamma_s - \gamma) + \tau_0^2 C_3/\nu^2\rho \qquad (2.17)$$

where $C_3 = K(1 - \tau_c/4)(h^2 + 0.0625 d^2)$. Now, for incipient motion, clearly $\tau_c = \tau_0$ so that Equation (2.17) reduces to

$$\tau_c^2 - B''\nu^2\rho\,\tau_c - B'\nu^2\rho\, d(\gamma_s - \gamma) \qquad (2.18)$$

where $B'' = 1/C_3$ and $B' = C_1/C_3$

For a particular sediment in a particular fluid, the equation reduces to a simple quadratic with only two coefficients to be evaluated experimentally. Equation (2.18) is assumed valid for Case I and for Case II. Certain difficulties remain but for the present we assume simply that the constants C_3 and B' are not the same for both Case I and II. This is considered later.

To obtain a similar expression applicable to Case III, we substitute Equation (2.16) into Equation (2.4) and have

$$\tau_c = \tau_s + F_{s/A_b} = \left[C_1 d(\gamma_s - \gamma) - \tau_c C_2 (1.562)\, K\pi S\right] + 6.248\, K \tau_o S$$

or $$\tau_c = C_1 d(\gamma_s - \gamma) + C_4 \tau_o \qquad (2.19)$$

where $$C_4' = 6.248\, KS - 1.562\, C_2 K\pi S$$

therefore: $$\tau_c \equiv C_1' d(\gamma_s - \gamma) \qquad (2.20)$$

where $C_1' = \dfrac{C_1}{(1 - C_4')}$ and should be a constant for a given sediment in a given fluid. This completes the derivation of the theory and now gives us expressions for all three of the aforementioned cases. It should be duly noted that the equations derived thus far take no regard of the intensity of turbulence. This criterion is mentioned later and is considered separately.

2.6 Estimation of Constants in Equations (2.18) and (2.20)

Even though the nature of the coefficients under consideration defy exact analytical determination, some notions of their magnitudes can be achieved by making reasonable estimates of the terms therein. For example, in Equation (2.4) we can reason that $d/4 < \ell_w < d/2$ and that an estimate of $\ell_w = 3d/10$ is within reason. If this reasoning is

carried to the other distances such that $\ell_s = 2/3d$, $\ell_a = 8d/27$, $\theta = 20^\circ$, K = 1 and h = 0.326 d, we arrive at the following magnitudes as realistic approximations.

Sand Size B-T	Laminar Flow		Turbulent Flow
	B'	L''	C_t'
12	-5,000	200,000	0.020
16	-20,000	300,000	0.025
20	-50,000	800,000	0.030
30	-75,000	1,000,000	0.040
60	-100,000	2,500,000	0.050

It is important to mention that the magnitudes of the above coefficients can be deduced from other reasonable estimates of θ, K, h, and the ℓ distances. Reasonable magnitudes of the coefficients will result if any one suitable set of the estimated values of θ, K, h, and ℓ are used with all of the various sand sizes. Upon close analysis of the algebraic forms of the coefficients it is evident that the magnitudes are very sensitive to small changes in the moment arm distances. The above values have been rounded off and are only a rough approximation.

A comparison of the estimated values of these coefficients with the ones obtained experimentally is found in Chapter 6.

CHAPTER 3

EXPERIMENTAL ANALYSIS

3.1 General

The principle components of the experimental equipment were a converging channel with a settling basin, a recirculating piping arrangement, an orifice meter, a pitot-static tube, a universal indicator, and a very sensitive pressure-cell.

3.2 Channel

The channel was constructed of quarter-inch Plexiglas. The joints were all milled and ground. During the construction, the unit was held together by tapped screws similar to flanged joints. Finally the joints were all glued with Testor's "Cement for Plastics" and a heavy duty Rohm and Haas "Cement PS-18." All of the joints were relatively square and there were no leaks whatsoever. The Plexiglas material permitted ample light for the visual observations. The convergent part of the channel emptied into the settling basin. Various screens and grillworks were used at the entrance to provide the desired entrance conditions. The channel was isolated from the pump vibrations by means of flexible couplings. The physical details are shown in Figure 4A.

3.3 Piping Arrangement

The pipes were all of a galvanized commercial two-inch type except for the flexible couplings which were made from industrial

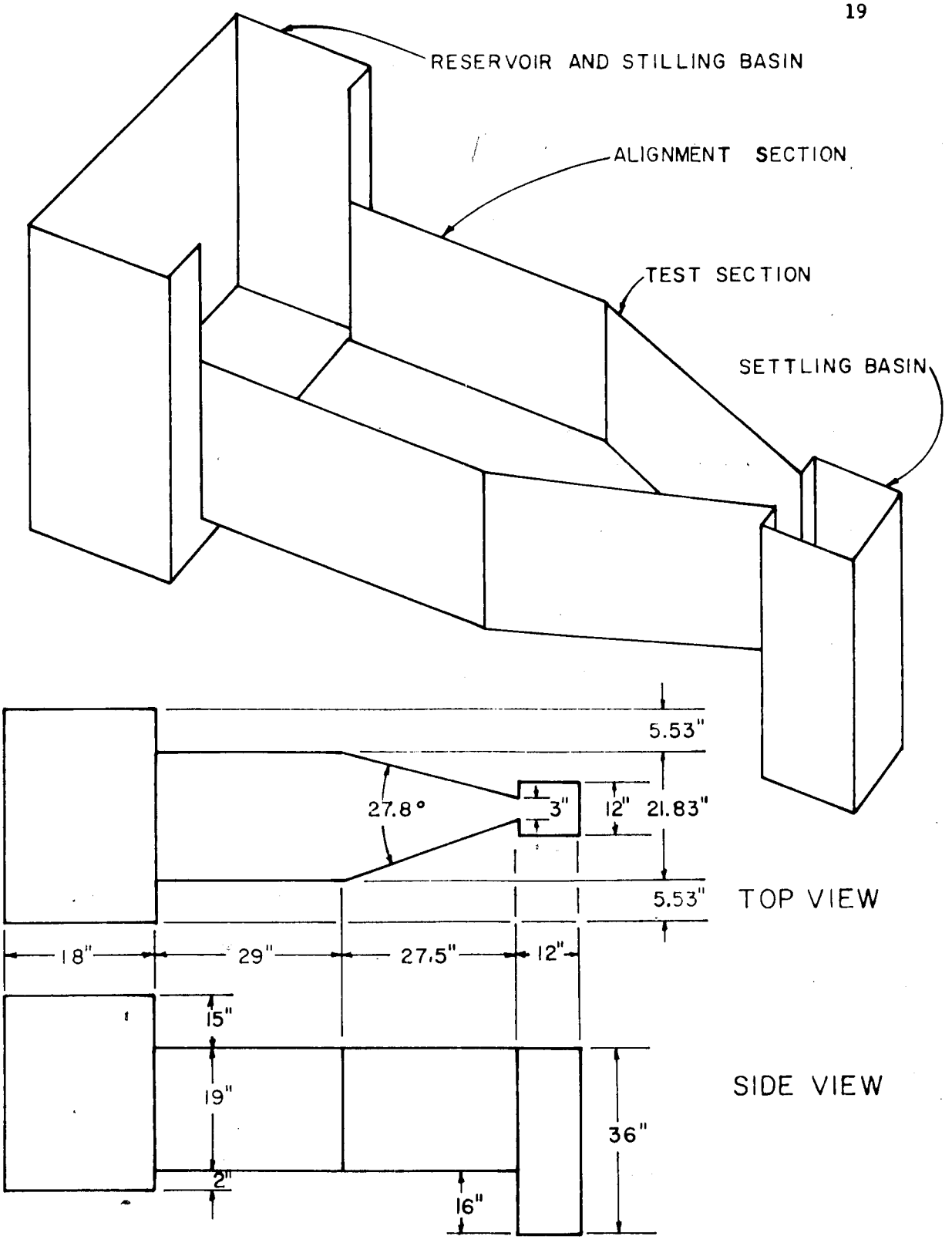

FIGURE 4A— EXPERIMENTAL CHANNEL

reinforced rubber hose. The calibration pipe was made from a two-inch Plexiglas tube. It was split with a band saw, with the aid of a special jig, flanged, glued with a given roughness, and then bolted back together with a gasket that just compensated for the saw-cut space. The interior of the tube was uniformly coated with a Baker-Thomas number 60 sand and had the appearance of sandpaper. The details of the tube and other particulars are shown in Figure 4B. The pump was an "Allis Chalmers Electrifugal" type and had a capacity of 100 gpm. The orifice-plate was a one-inch square-edged type and was very sensitive even at low flows.

3.4 Pitot-Static Tube

This instrument was made from a brass electrode tube, and standard commercial brass fittings. It was carefully calibrated in the plexiglas tube and then subsequently placed in the channel for the shear measurements after the fashion of Preston, Hsu, and Laursen and Hwang. The tube had an outside diameter of 0.0425 inches and an inside diameter of 0.0215 inches. See Figure 5 for the details of the tube.

3.5 Electronic Instrumentation

The pitot-static tube was attached to a Statham $\pm$ 0.01 psid pressure cell. The indicating instrument was a null balancing type. It was a new transistorized unit and had high amplification. A Hewlitt-Packard Oscilloscope was also used to monitor the strains and permit a closer control on the measurements.

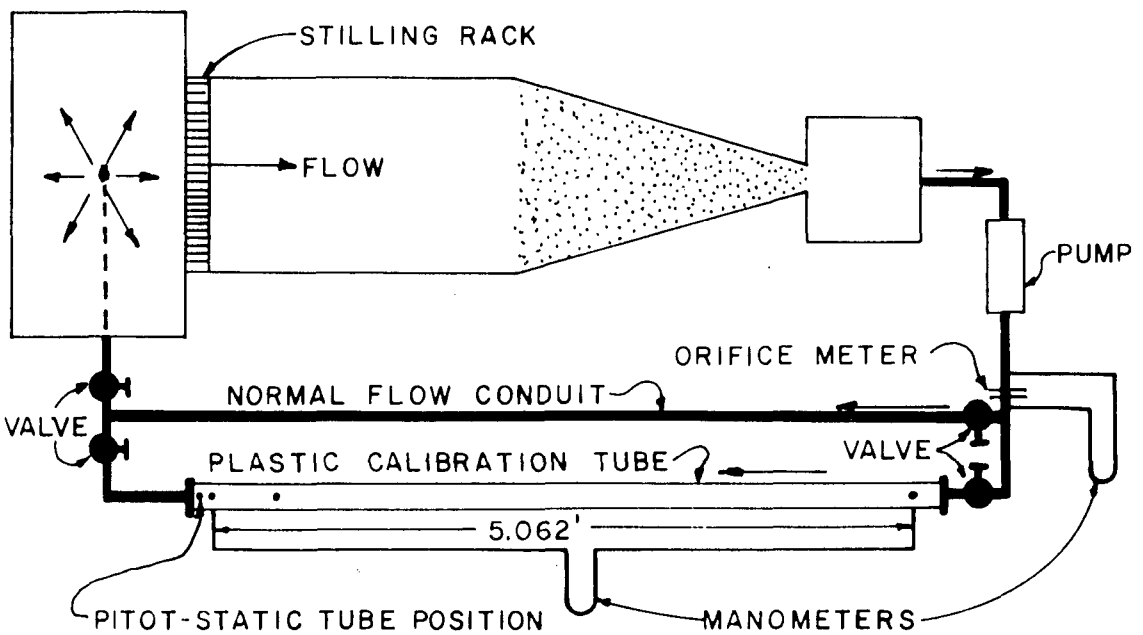

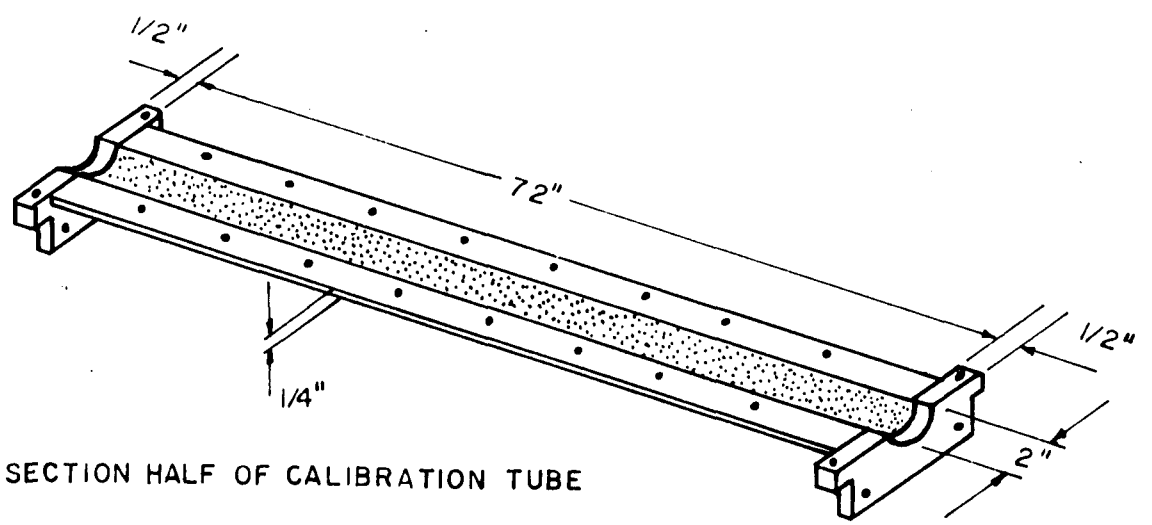

SECTION HALF OF CALIBRATION TUBE

FIGURE 4B —— PIPING ARRANGEMENT

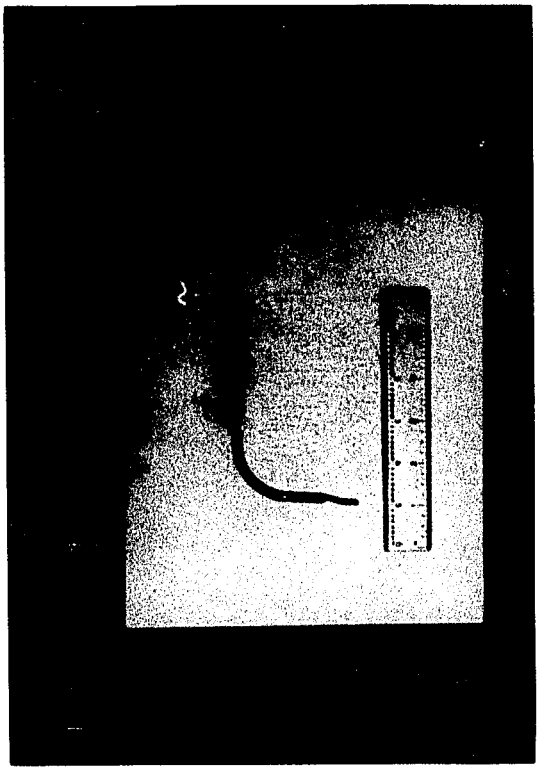

FIGURE 5 -- PITOT-STATIC TUBE

CHAPTER 4

EXPERIMENTAL PROCEDURE AND SCOPE OF THE INVESTIGATION

The purpose of the experiment was to measure the critical tractive stress, τ_c , under conditions of laminar and turbulent flow. Evidence of a transition region between the two was also sought. This is discussed in Chapter 6.

4.1 Preliminaries

Orifice meter calibrations were performed carefully according to the usual procedures. These calibration curves are presented in Figure 7. The pitot-static tube for the shear measurements was calibrated in the split plastic tube which had been designed for that purpose. It was coated with a Baker-Thomas number 60 sand. This work checked that of Laursen and Hwang quite well (See Figure 8). Thereafter their curves were used for the other particle sizes. This calibration was meticulously performed since the success of the entire experiment depended upon it.

4.2 Obtaining Data

Three fluids--water, oil, and kerosene--were used in the experimental program.

Water was taken from the city supply and the viscosity was found to be the handbook values. All of the experiments with water were completely within the turbulent regime. That the flow was turbulent was determined by a dye filament injected upstream at various depths. The Reynolds numbers, based on D=4R and average velocity, ranged from 7,000

to about 50,000. The flow rate varied from 0.007 cfs to about 0.20 cfs and depths from 0.30 in. to 3.5 in. Water temperatures varied about 15 degrees Fahrenheit during any one run.

The laminar part of the experiment was performed with a non-detergent oil, "Shellectric," which had a viscosity about ten times that of water. See Figure 9 for the manufacturer's specifications. The oil tests were totally within the laminar regime, demonstrated by dye streaks injected upstream. Reynolds numbers varied from about 200 to 1,000. Flow rates varied from 0.01 cfs to about 0.10 cfs. Depths ranged from 0.25 in. to 2.5 in. The temperatures ranged over about 22 degrees Fahrenheit during most of the runs.

A high quality kerosene, "Chevron Pearl," proved to have the right properties to yield measurements within both regimes of flow. The viscosity was determined to be very close to handbook specifications. The values of the Reynolds numbers ranged from about 1,400 to 3,000 in the laminar regime and from about 3,000 to 20,000 in the turbulent regime. Flow rates varied from about 0.01 cfs to 0.14 cfs. Dye filaments were again utilized to ascertain the flow regime.

4.3 Testing Procedure

For the water, oil, and kerosene experiments, the following procedure was employed:

1. The particular sand was placed in the test section as evenly and smoothly as possible. A light coating of colored particles was sprinkled over the surface. The pump was started and a flow maintained that just caused the particles to move in the downstream end where the velocity and shear were highest.

2. The shear stress was measured at the point of the impending motion by means of the Preston technique. The most upstream point of the incipient motion was determined by noting that the colored surface particles had moved leaving a line of acceptable distinction where the shear stress could then be measured. The stresses had to be measured as soon as a stable condition existed because of scouring action that soon distorted the downstream configuration. When the shear stresses were measured the position of the tube was not critical since slight changes in location did not significantly affect the pressure readings. The flow was increased and the point of incipient motion moved upstream where the stresses could again be measured. As the point of incipient motion moved upstream it was found that the intensity of critical shear stress remained the same.

3. The laminar flow regime question was solved by means of dye filaments injected upstream. Food coloring was used with the water tests, while a purple oil, "Royal Triton," was used with the oil and kerosene experiments. The dye streaks were injected at various positions from close proximity to the channel floor to very near the free surface.

4. A coarse screen was placed just upstream from the position of critical shear stress in an effort to determine the effects of increased turbulence. Evidently the turbulence level at the channel floor was only slightly affected. No noticeable differences in the shear stresses could be detected as a result of the presence of the screen.

4.4 Sand-Type Employed

The sand used in this experiment was obtained commercially from a local firm, Baker-Thomas and Company. This sand was uniform. The average grain size was of some question but a sieve analysis was made and the results are presented below so that no confusion can exist. The sand is used commercially for filtering purposes and was originally quite clean.

Baker-Thomas Commercial Size	Average Diameter (ft)
12	0.0058
16	0.0038
20	0.0023
30	0.0013
60	0.0007

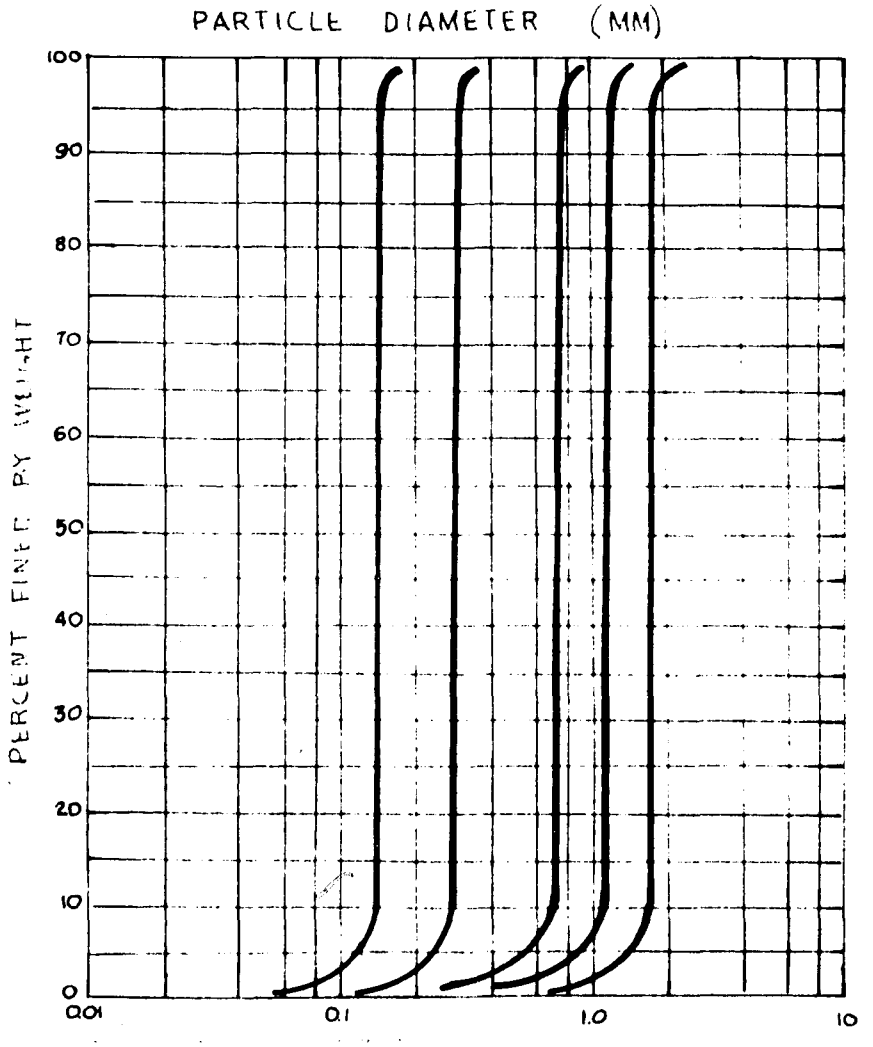

FIGURE 6--GRAIN SIZE DISTRIBUTION CURVE

CHAPTER 5

DATA EVALUATION

During the preliminary runs it was quickly apparent that the most difficult part of the analysis would be the shear measurements. The exact positon of the tube, vertically and horizontally, was subject to the visual alertness of the observer. However, the clear walls of the channel and good lighting increased the visibility. Several observers were queried and all seemed to note about the same position of the tube. Fortunately the tube position could be varied slightly and the pressure readings were not significantly altered. Resulting magnitudes of the shear stresses tended to be about the same for small ranges of pressure differentials due to the large slope of the calibration curves.

5.1 Computation of Variables

Velocity. Velocities in the test section were computed from the arc that represented the flow area. The fundamental equation of continuity was used.

Shear. The shear measurements were the most important part of the analysis. They were determined from the pitot-static tube pressure differentials and values from the calibration curves of Laursen and Hwang. Besides the difficulties mentioned by Laursen and Hwang (8) minor problems existed with a slight hysteresis of the pressure cell which amounted to about 0.01 percent.

5.2 Dimensionless Parameters

In this analysis several dimensionless parameters are utilized. They are $\tau_c/d\Delta\gamma$, and $d/\delta' = \frac{d}{11.6\nu}\sqrt{\tau_o/\rho}$. These are the ones presented by Shields in his classical analysis and would be obtained from a dimensional analysis procedure assuming that τ_c was dependent only upon d, $\Delta\gamma$, and δ'. This assumption implies that the resisting force is dependent upon the submerged weight of the particle and that the impelling force due to the flow around the particle is dependent on a flow which is within the law of the wall. From the discussion and analysis of results in Chapter 6 it will be seen that these dimensionless terms are evidently the ones of significance.

5.3 Sample Calculations

Sample calculations are presented for each of the dimensionless parameters. In each case the American engineering system of units is used. The data comes from the first run. See Table I.

$$\tau_c/d\Delta\gamma = 0.0149/(0.0058)(62.4)(2.65-1) = 0.0250$$

$$d/\delta' = [0.0058/11.6(1.059)(10^{-5})]\sqrt{\frac{0.0149}{1.935}} = 4.40$$

5.4 Errors

Errors are an interesting part of any experimental analysis. The errors of importance are those associated with the shear measurements. The degree to which numerical data tend to spread about an average value can be expressed in several ways. One of the most common and meaningful methods is by means of the so-called "standard error" which is the same as the well-known standard deviation when the deviations are measured

from the mean value. A table of the standard errors for the shear measurement data, expressed in percent, is presented below for the water and oil phases of the investigation.

Sand Size	Standard Error	
B.T. No.	Laminar	Turbulent
60	1.1%	0.90%
30	1.4%	1.2%
20	2.6%	2.2%
16	4.9%	3.1%
12	6.8%	5.4%

It is immediately noticeable that the standard error increases with the size of the roughness. The error is also slightly greater with laminar flow than with turbulent flow. The increasing error with size is possibly due to a greater sphericity of the smaller sand particles and a subsequently more distinctive rolling action than the more unstable larger grains. The laminar flow errors are possibly greater because of the physical difficulties with the oil, such as a longer equilibrium time, a less distinctive point of critical shear stress, and a tendency of the oil to discolor.

CHAPTER 6

RESULTS AND CONCLUSIONS

6.1 Analysis of Results

The Preston technique of shear measurement is evidently well suited for open channel applications, as suggested by Laursen and Hwang (8). The experimental results, tabulated in Table I, indicate a reasonable degree of consistency with the shear measurements. Shear measurements can be made easily and simply with standard electronic indicators and a sensitive pressure transducer. That the shear measurement technique will be helpful in many fluid flow experiments is evidenced by the success of this investigation.

Several conclusions can be reached from the experimental results. First, a comparison with the work of Shields and White is of interest. Figure 10 shows the work of those investigators on the same plot with the results obtained from this investigation. It is immediately noticeable that the magnitudes are all of the same order but that there are important differences.

Shields' work was extrapolated from the bed-load transport curve to the time that bed-load ceases. This procedure could easily yield values that were erratic due to the very nature of the bed-load transport curve. Perhaps the bed condition of Shields' apparatus was composed of ripple formations. If so, the critical shear would be higher because a part of the total shear is the "horizontal" component of the pressure

distribution on the ripples. These reasons might serve to explain the comparatively higher values of Shields' data. The one-to-one laminar line that is placed on most Shields' diagrams is questionable because no data justifies it. No evidence to suggest such a line was found in this investigation.

Most of White's runs involved some movement of the bed particles rather than the exact condition of incipient motion. The shear stresses thus obtained should be slightly higher than the critical shear, depending upon how much transport was involved. A comparison with White's data bears this out. White's laminar flow data shows a series, with the same size sand, which is described as: general movement, 1% of top grains moving, very few grains move, and movement begins. The measured shear decreased in this order and only the last condition should be compared with the laminar results of this investigation. This difference is not great and might be due to differences in measuring techniques. The turbulent data of White is not as well described as the viscous data. Possibly movement had already begun and if so, the higher stresses are understandable. In both the laminar and turbulent flow White's values are above the values found in this investigation. The ratio between the laminar and turbulent critical, however, are in good agreement.

At the beginning of this investigation it was believed that a transition between laminar and turbulent conditions should exist as in the surface resistance problem. The water and oil experiments did not reveal a transition and a considerable overlap of values of the ratio of the particle diameter to the nominal laminar sub-layer was found.

This discontinuity was studied further by performing several additional runs with kerosene, which permitted flows in both the laminar and turbulent regimes. The expected transition between the laminar and turbulent cases could not be detected. Since the sequence of runs had to progress from the laminar to the turbulent state, and the critical laminar shear was greater than the turbulent, the possibility of a sudden transition cannot be completely ruled out. Similarly the stability of the contracting flow would tend to shorten the transition region if it exists. However, the transition usually found in surface resistance experiments could be the result of averaging a mixture of laminar and turbulent states over a larger area.

Size correlates very well with the critical tractive shear stress, as seen in Figure 11. The discontinuous correlation in the two flow regimes is evident in the plot. A similar discontinuity exists in all of the results. The turbulent data presented here should be directly applicable for design purposes. The turbulent screen effects lead to a conclusion that small changes in the magnitude of the turbulence of the ambient flow do not appreciably affect the critical shearing stress.

6.2 Experimental Verification of Analytical Formulas

The analytical formulas (2.18) and (2.20) are reasonably verified by the experimental results. The values of the coefficients vary with the sediment diameter and do not remain constant from size to size. The table below indicates the experimental coefficients for the various sand sizes.

SEDIMENT Size (B-T)	COEFFICIENTS				
	Laminar		Turbulent		
	B'	B''	C'	*B'	*B''
60	-101,216	2,527,952	0.0353	---	---
30	-73,707	1,229,090	0.0335	---	---
20	-47,884	719,550	0.0326	-464,221	7,164,998
16	-18,672	314,929	0.0274	-281,642	5,166,881
12	-4,499	114,661	0.0252	-104,602	2,166,451

*Values in these columns apply to Case II

The values in the table are self-explanatory and are presented to clarify the results. It is interesting to compare the experimental coefficients with the estimated ones at the end of Chapter 2. There is close agreement between the two sets of coefficients. A plot of the two sets is presented in Figure 12. The good agreement between analysis and measurement permits a possible conclusion that the assumptions made in the analytical derivations are justifiable, i.e. that the logarithmic velocity distribution is at least a good approximation near the boundary, and the law of the wall is a good estimate of the conditions there, and that drag force is expressible as an integral. The ℓ distances in the equilibrium equations might be questionable but various combinations of reasonable estimates give essentially the same resulting magnitudes. That their relative position for various size particles does not change is not unreasonable and, if so, then the analysis predicts that $\frac{\tau_c}{d\Delta\gamma}$ should vary with size, which is borne out by the experimental results.

6.3 Summary of Conclusions

1. The critical tractive force relationships, as determined from the measurements, plots as a discontinuous function of $\tau_c/d\Delta\gamma$ versus

d/δ'. No evidence of a transitional function between the laminar and turbulent regimes was found.

2. The approximate analysis confirms the experimental findings qualitatively. The numerical magnitudes of critical tractive force as predicted from the analysis are very sensitive to small changes in the assumed flow conditions around the particle. However, the agreement between analysis and experiment is entirely reasonable.

3. The discrepancies between the values obtained in this investigation and those of White and Shields are explainable; the primary differences being the result of measurement techniques. The results reported herein give tractive force magnitudes that are somewhat less than previously found, but are very consistent and are the result of more precise measurement techniques.

APPENDICES

TABLE I

DATA RUN SUMMARY

Run No.	d_s (ft.)	Fluid	Avg. Temp. °F	V_c ft/sec	τ psf	$\tau_c/d\Delta\gamma$	d/δ'
1	0.0058	Water	75	1.52	0.0149	0.0250	4.40
2	0.0058	Water	74	1.51	0.0151	0.0253	4.43
3	0.0058	Water	73	1.46	0.0150	0.0250	4.41
4	0.0058	Water	80	1.52	0.0151	0.0252	4.42
5	0.0058	Water	81	1.50	0.0150	0.0253	4.43
6	0.0038	Water	71	1.22	0.0112	0.0276	2.39
7	0.0038	Water	72	1.18	0.0107	0.0274	2.30
8	0.0038	Water	73	1.15	0.0106	0.0280	2.26
9	0.0038	Water	76	1.15	0.0106	0.0270	2.30
10	0.0038	Water	77	1.16	0.0115	0.0115	2.31
11	0.0025	Water	75	1.15	0.0081	0.0313	1.39
12	0.0025	Water	80	1.11	0.0083	0.0314	1.42
13	0.0025	Water	79	1.13	0.00814	0.0314	1.40
14	0.0025	Water	84	1.13	0.00839	0.0317	1.41
15	0.0025	Water	85	1.13	0.00846	0.0324	1.42
16	0.0013	Water	76	1.041	0.00433	0.0328	0.529
17	0.0013	Water	74	1.06	0.0044	0.0336	0.533
18	0.0013	Water	76	1.05	0.0044	0.0332	0.532
19	0.0013	Water	76	1.05	0.0048	0.0331	0.532
20	0.0013	Water	77	1.04	0.0044	0.0340	0.539
21	0.0007	Water	74	0.98	0.00255	0.0353	0.216

Run No.	d_s (ft.)	Fluid	Avg. Temp. °F	V_c ft/sec	τ psf	$\tau_c/d\Delta\gamma$	d/δ'
22	0.0007	Water	79	0.97	0.00260	0.0358	0.220
23	0.0007	Water	72	0.96	0.00244	0.0359	0.213
24	0.0007	Water	79	0.95	0.00255	0.0353	0.219
25	0.0007	Water	91	0.97	0.00257	0.0353	0.218
26	0.0058	Oil	90	1.206	0.0641	0.0999	0.452
27	0.0058	Oil	91	1.21	0.0642	0.0984	0.453
28	0.0058	Oil	94	1.16	0.0643	0.0980	0.450
29	0.0058	Oil	96	1.20	0.0640	0.0981	0.451
30	0.0058	Oil	94	1.18	0.0641	0.0999	0.452
31	0.0038	Oil	89	1.12	0.0471	0.112	0.257
32	0.0038	Oil	90	1.07	0.0470	0.112	0.257
33	0.0038	Oil	92	1.07	0.0471	0.113	0.256
34	0.0038	Oil	94	1.07	0.0471	0.112	0.255
35	0.0038	Oil	98	1.10	0.0467	0.110	0.256
36	0.0025	Oil	95	1.03	0.0322	0.115	0.137
37	0.0025	Oil	98	1.02	0.0322	0.117	0.138
38	0.0025	Oil	99	1.03	0.0328	0.117	0.138
39	0.0025	Oil	101	1.03	0.0326	0.116	0.138
40	0.0025	Oil	96	1.02	0.0327	0.117	0.139
41	0.0013	Oil	82	0.888	0.0166	0.115	0.052
42	0.0013	Oil	84	0.901	0.0164	0.114	0.052
43	0.0013	Oil	86	0.898	0.0164	0.114	0.052
44	0.0013	Oil	88	0.914	0.0164	0.115	0.052

Run No.	d_g (ft.)	Fluid	Avg. Temp. °F	Vc ft/sec	τ_o psf	$\tau_o/d\Delta\delta$	d/δ'
45	0.0013	Oil	82	0.904	0.0166	0.115	0.052
46	0.0007	Oil	97	0.813	0.00926	0.1197	0.0231
47	0.0007	Oil	90	0.813	0.00926	0.1196	0.0231
48	0.0007	Oil	92	0.811	0.00925	0.1194	0.0230
49	0.0007	Oil	94	0.817	0.00926	0.1195	0.0231
50	0.0007	Oil	96	0.817	0.00926	0.1197	0.0234
51	0.0058	Kerosene	76	---	0.0233	0.080	3.33
	0.0058	Kerosene	73	---	0.0194	0.030	2.40
52	0.0058	Kerosene	77	---	0.0534	0.081	3.34
	0.0058	Kerosene	79	---	0.0193	0.029	2.39
53	0.0058	Kerosene	81	---	0.0532	0.079	3.32
	0.0058	Kerosene	82	---	0.0195	0.031	2.41
54	0.0038	Kerosene	72	---	0.0535	0.082	1.30
	0.0038	Kerosene	73	---	0.0197	0.030	1.60
55	0.0038	Kerosene	74	---	0.0534	0.081	1.29
	0.0038	Kerosene	76	---	0.0193	0.029	1.59
56	0.0038	Kerosene	78	---	0.0536	0.082	1.31
	0.0038	Kerosene	76	---	0.0192	0.028	1.58
57	0.0007	Kerosene	78	---	0.0111	0.0996	0.094
	0.0007	Kerosene	78	---	0.00298	0.0370	0.098

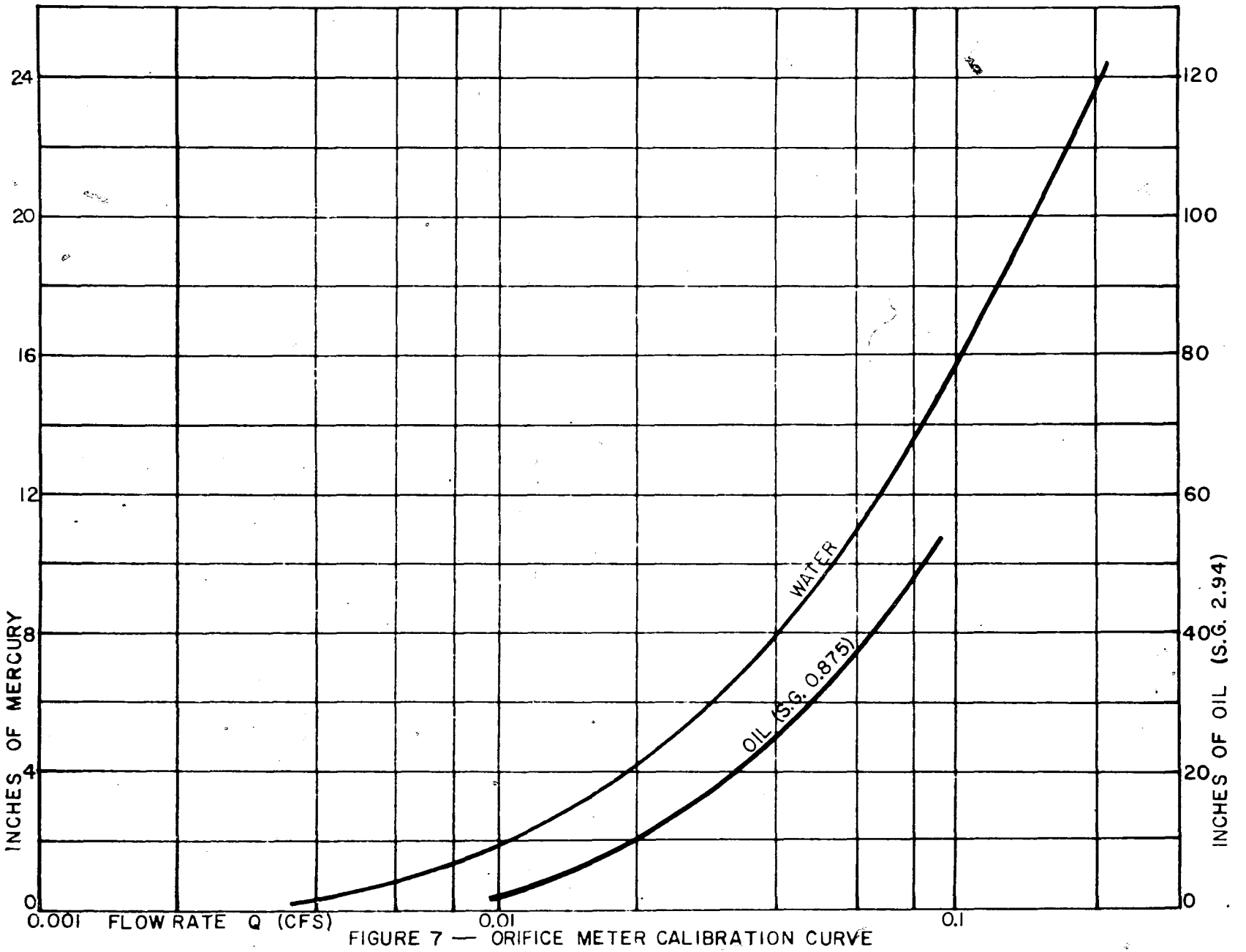

FIGURE 7 — ORIFICE METER CALIBRATION CURVE

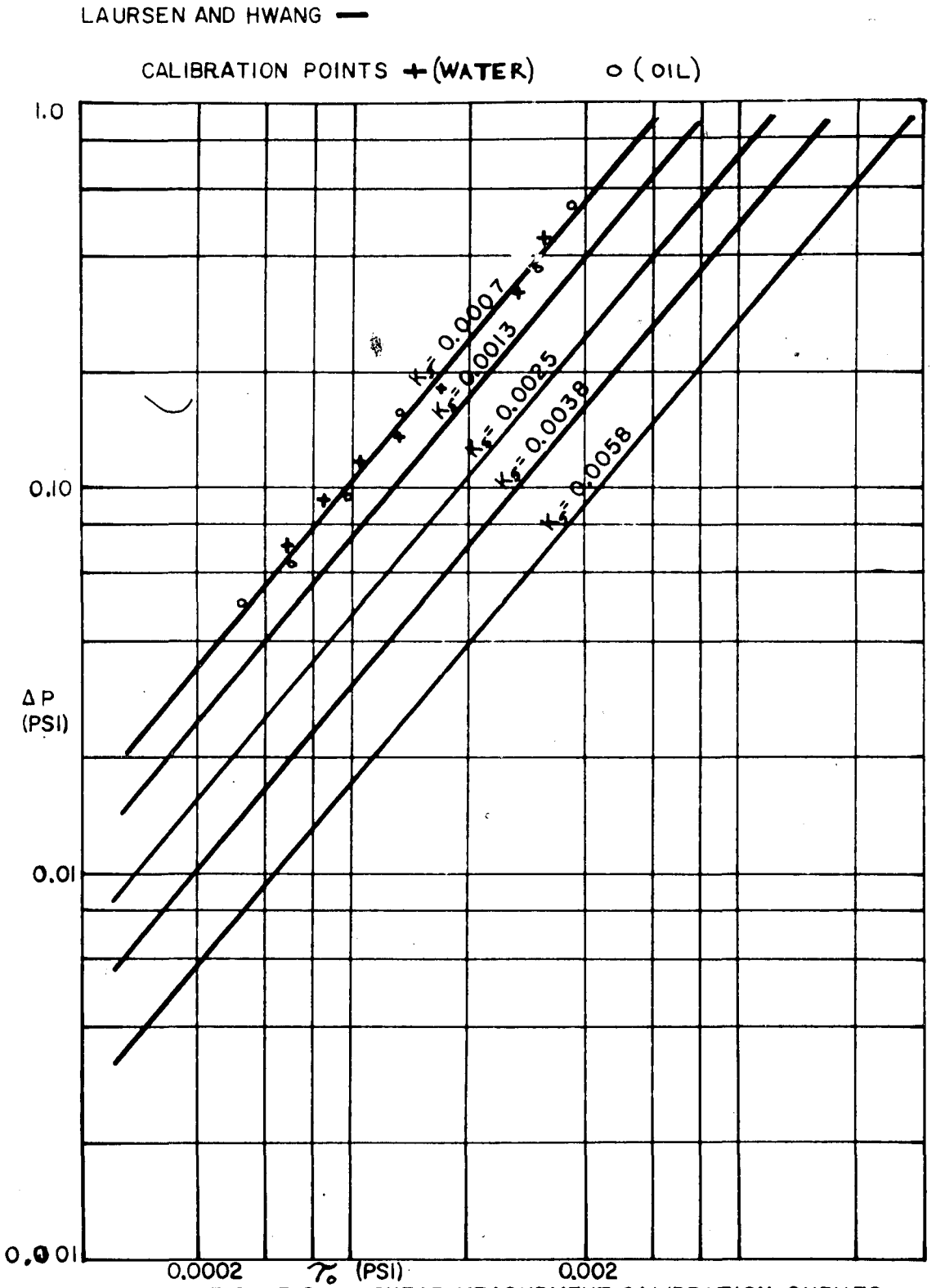

FIGURE 8 — SHEAR MEASURMENT CALIBRATION CURVES

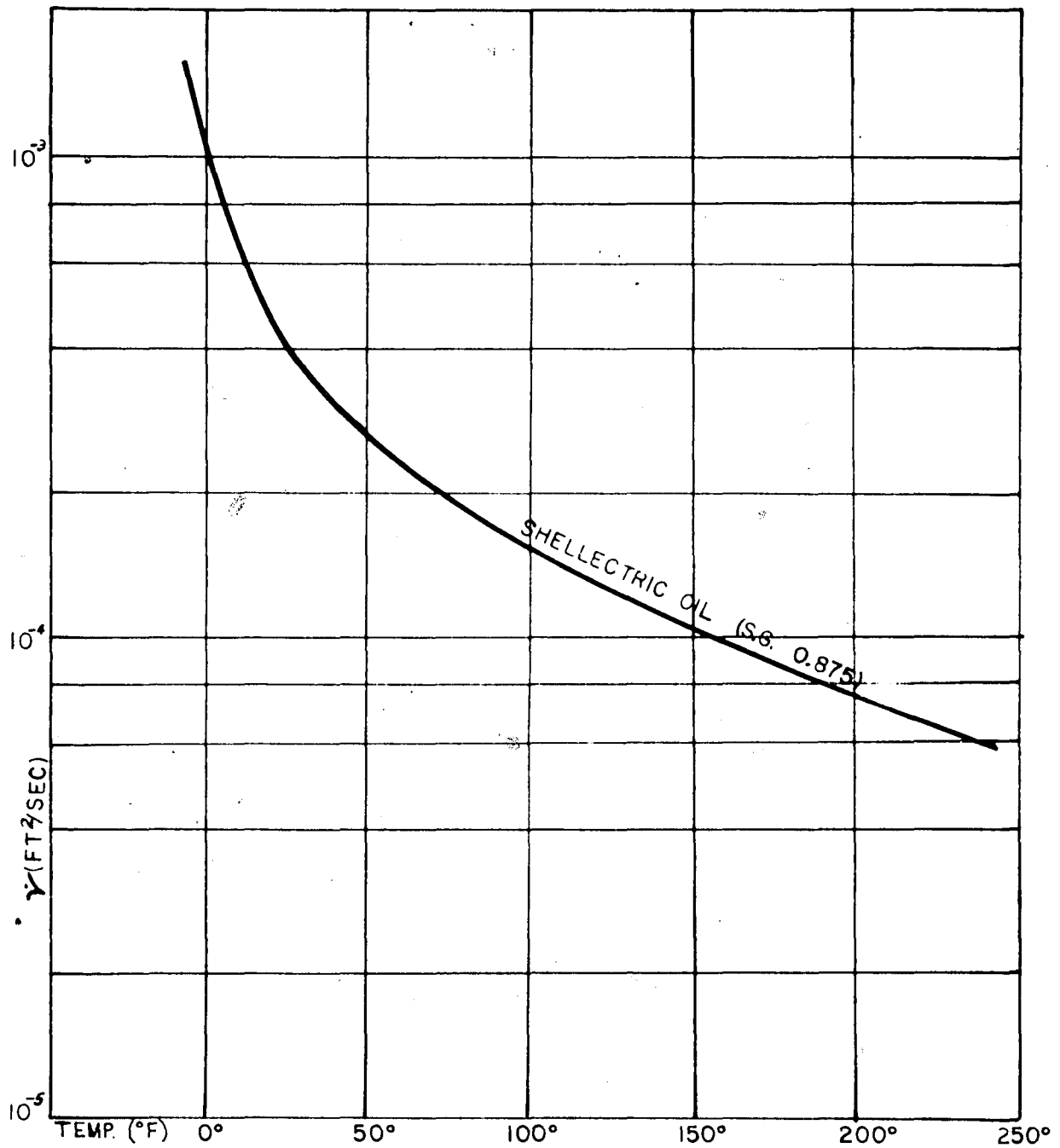

FIGURE 9 — MANUFACTURER'S SPECIFICATIONS

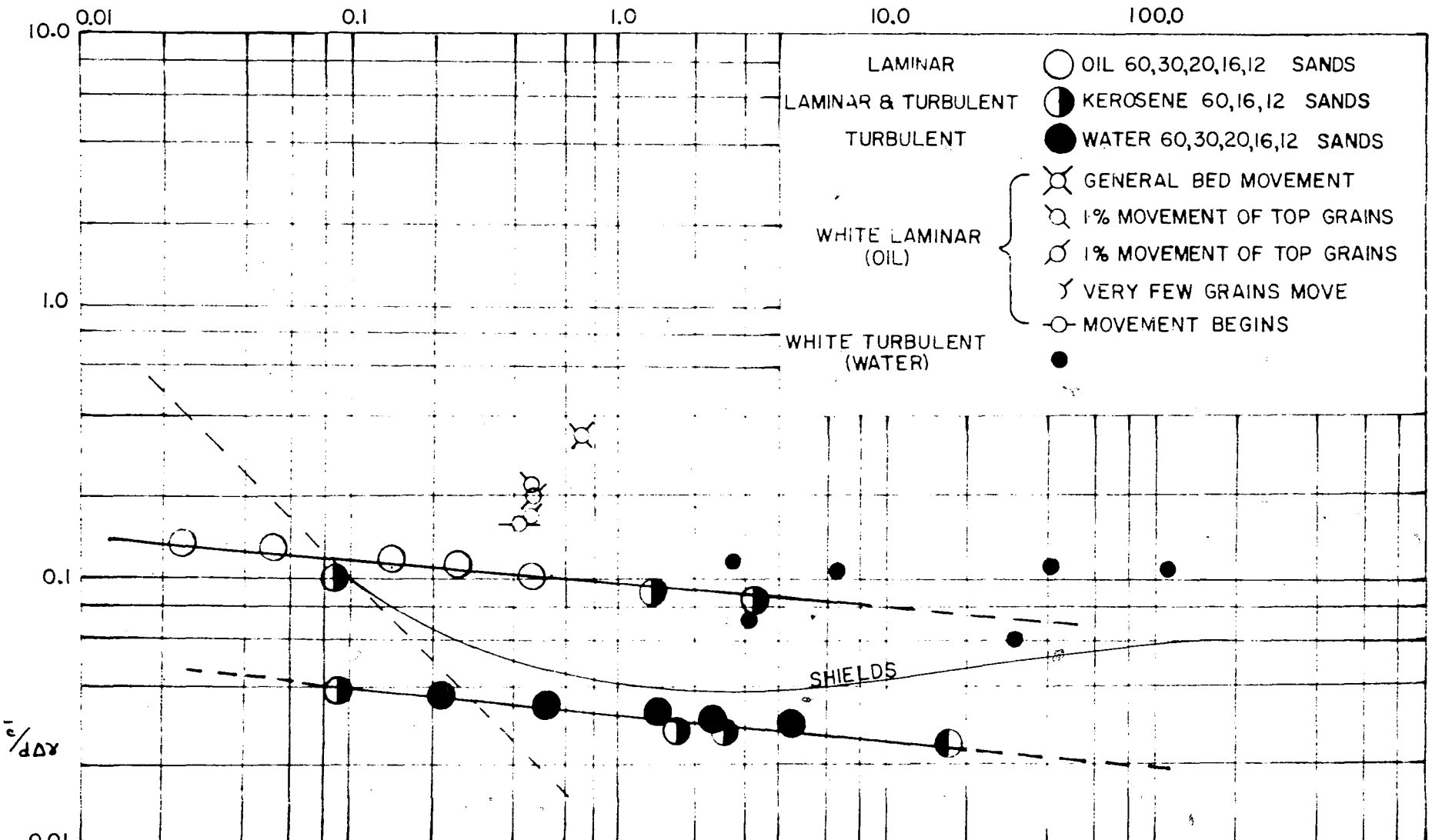

FIGURE 10 — SHIELDS DIAGRAM

(The notation of Figure 11 is the same as that of Figure 10)

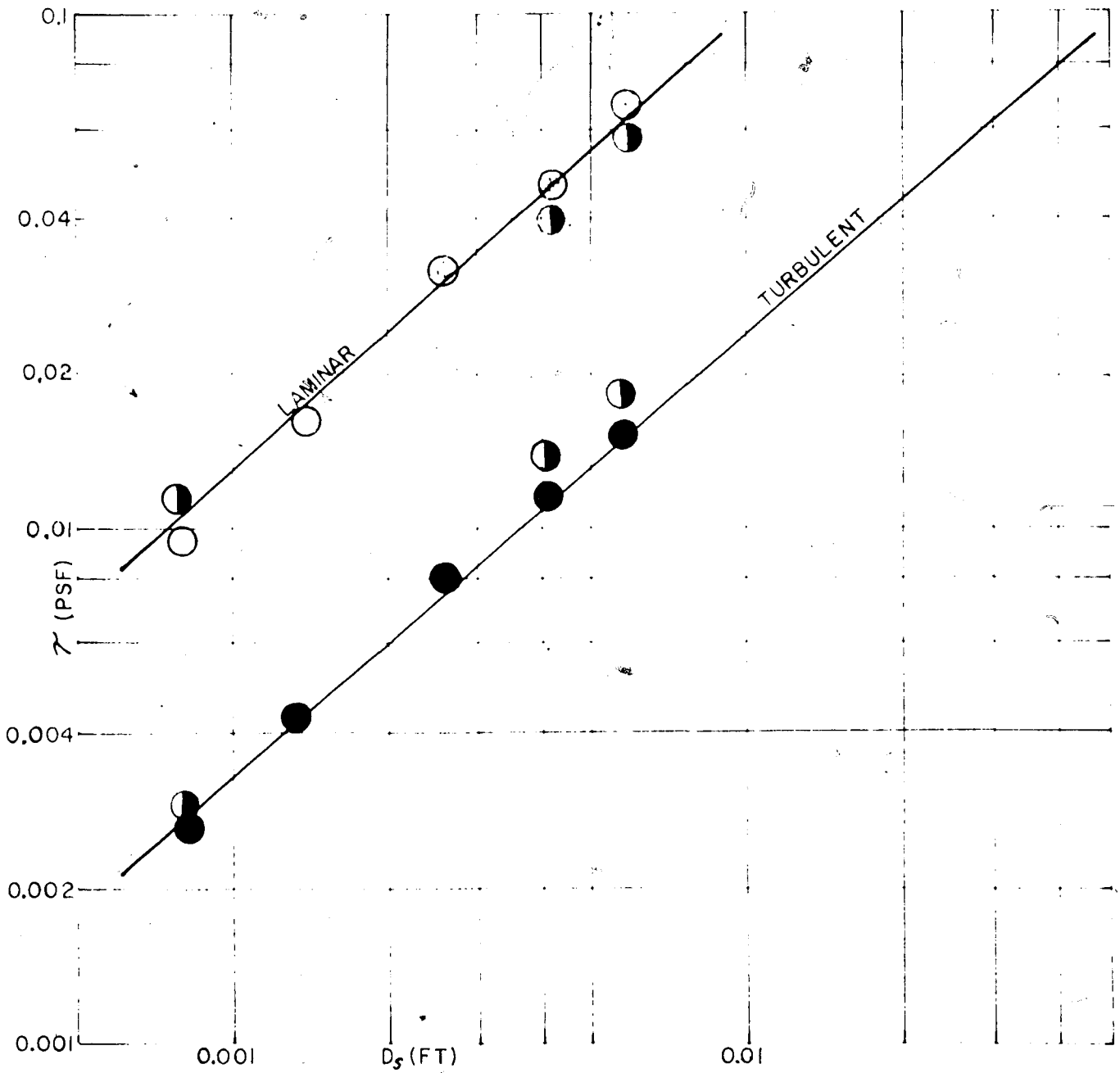

FIGURE 11 — τ VS SIZE

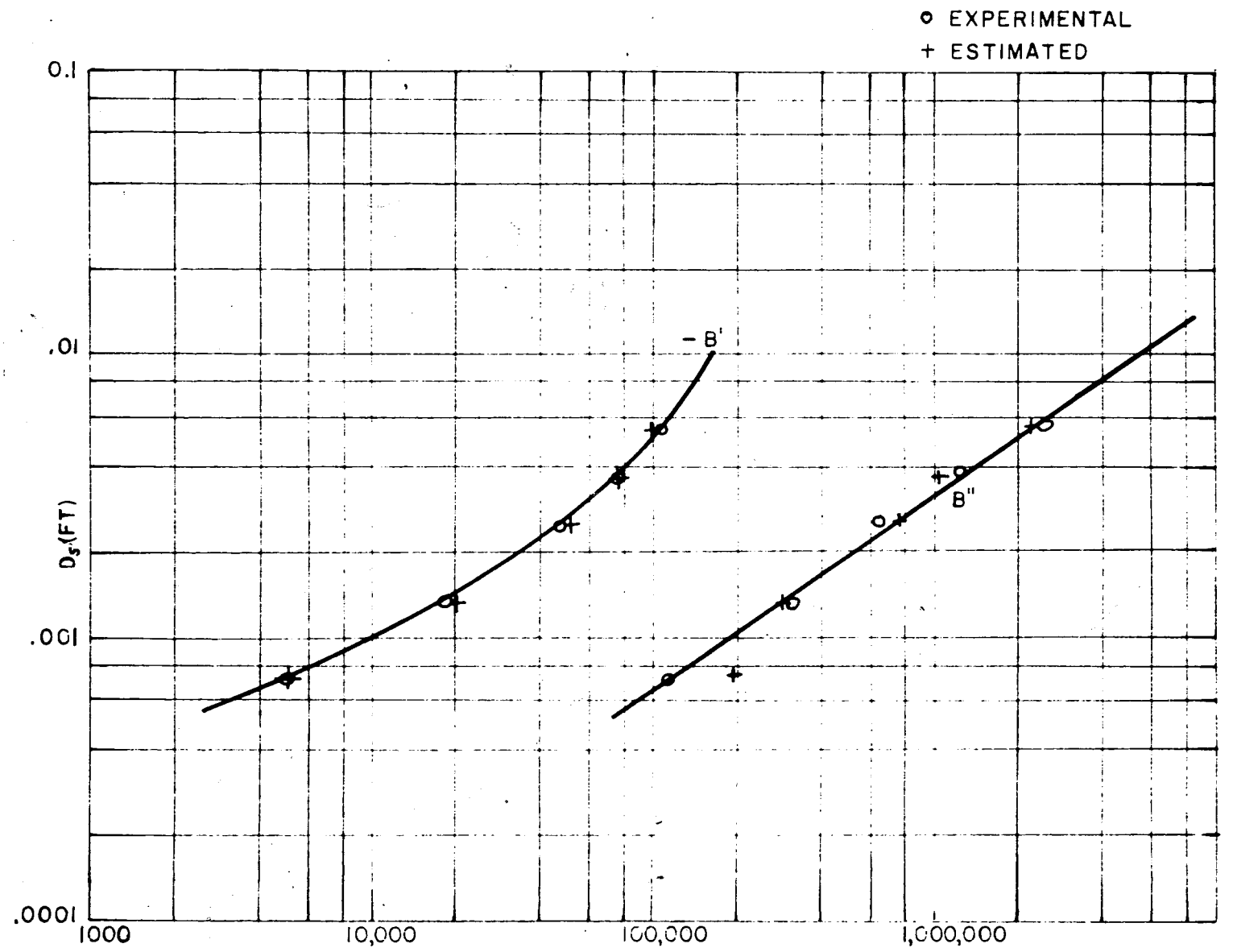

FIGURE 12A— SIZE VS COEFFICIENTS

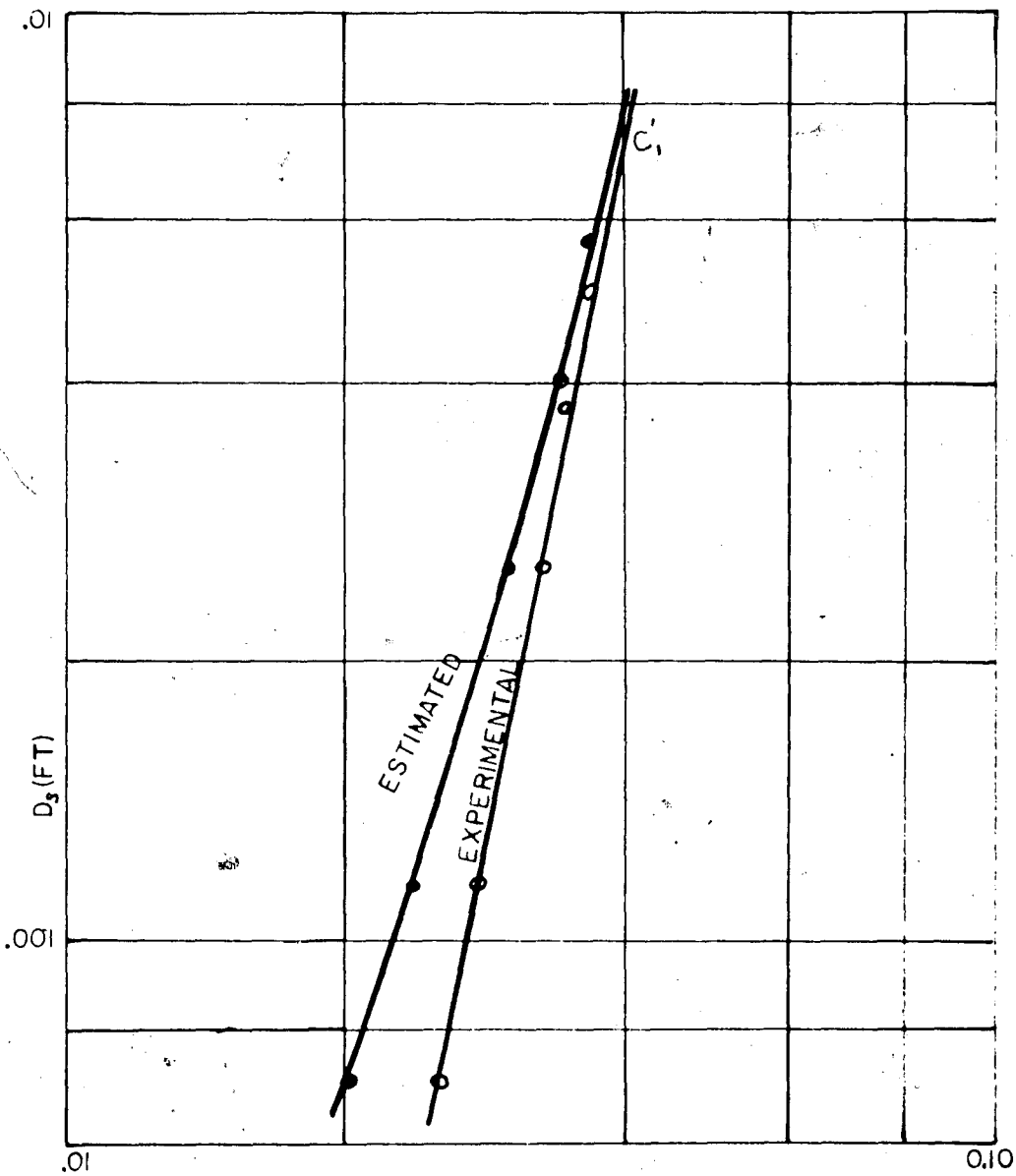

FIGURE 12B— SIZE VS COEFFICIENTS

BIBLIOGRAPHY

(1) Kempf, G., "Neue Ergebnisse der Widerstandsforschung," Werft, Reederei, Hafen, 10, 1929.

(2) Schultz-Grunow, F., "New Frictional Resistance Law For Smooth Plates," N.A.C.A. Technical Memorandum 986, 1941.

(3) Liepmann, H. W. and Dhawan, S., "Direct Measurements of Local Skin Friction in Low Speed and High Speed Flow," Proceedings First U. S. National Congress for Applied Mechanics, Chicago, 1951. See also Dhawan, S., "Direct Measurements of Skin Friction," N.A.C.A. Technical Note 2567, 1952.

(4) Fage, A. and Falkner, V. M., "An Experimental Determination of the Intensity of Friction on the Surface of an Aerofoil," Aeronautical Research Committee (Great Britain) Reports and Memoranda 1315, 1930.

(5) Ludweig, H. "Instrument for Measuring the Wall Shearing Stress of the Turbulent Boundary Layer," Ing. Archiv., Vol. 17, No. 3, 1949. Translated as N.A.C.A. Technical Memorandum 1284, 1950.

(6) Preston, J. H. "The Determination of Turbulent Skin Friction by Pitot Tubes," Journal of Royal Aeronautical Society 110, Vol. 58, 1954.

(7) Hsu, E. Y., "The Measurement of Local Turbulent Skin Friction By Means of Surface Pitot Tubes," David W. Taylor Model Basin Research and Development Report No. 957, 1955.

(8) Laursen, E. M., and Hwang, L. S., "Extension of Preston's Shear Measurement Technique to Rough Boundaries," Technical Report No. 1, NSF G-7409, National Science Foundation, 1962.

(9) White, C. M., "Equilibrium of Grains on Bed of Stream," Proceedings Royal Society of London, Vol. 174A, 1940.

(10) Shields, A., "Anwendung der Aeknlichkeitsmechanik und der Turbulenz-Forschung auf die Geschiebewegung," Mitteilungen der Preuss. Vercuchsanst. f. Wasserbau u. Schiffbau., Berlin, Heft 26, 1936.

(11) Kalinski, A. A. and Hsia, C. H., "Study of Transportation of Fine Sediments by Flowing Water," University of Iowa Studies in Engineering, Bulletin 29, 1945.

(12) Rubey, W. W. "The Force Required to Move Particles on the Bed of a Stream," U. S. Geological Survey Paper 189E, 1938.

(13) Hjulstrom, P., "Transportation of Detritus by Moving Water," Recent Marine Sediments, Am. Association of Poeroleum Geologists, 1939.

(14) Glover, R. E. and Florey, Q. L., "Stable Channel Profiles," U. S. Bureau of Reclamation Hydraulic Laboratory Report No. Hyd. 325, 1951.

(15) Olsen, O. J. and Florey, Q. L., "Sedimentation Studies in Open Channels: Boundary Shear and Velocity Distributions by Membrane Analogy, Analytical and Finite Difference Methods," U. S. Bureau of Reclamation Hydraulic Laboratory Report No. Hyd. Sp-34, 1952.

(16) Carter, A. C. and Carlson, E. J., "Critical Tractive Forces on Channel Side Slopes," U. S. Bureau of Reclamation Laboratory Report No. Hyd. 295, 1953.

(17) Lane, E. W., "Design of Stable Channels," Transactions of the American Society of Civil Engineers, Vol. 89, 1926.

(18) Lane, E. W. and Carlson, E. J., "Some Factors Affecting the Stability of Canals Constructed in Coarse Granular Materials," Proceedings of the Minnesota International Hydraulics Convention, 1953.

(19) Lane, E. W., "Progress Report on Results of Studies on Design of Stable Channels," U. S. Bureau of Reclamation Hydraulic Laboratory Report No. Hyd.352, 1952.

(20) Rouse, Hunter, "Advanced Fluid Mechanics," John Wiley and Sons, New York, 1959.

(21) Vennard, J. K., "Elementary Fluid Mechanics," Fourth Edition, John Wiley and Sons, New York, 1962.

(22) Prandtl, Ludweig, "Fluid Dynamics," Hafner Publishing Company, New York, 1952.

(23) Ludweig, H., and Tillman, W., "Investigation of the Wall Shearing Stress in Turbulent Boundary Layer," Ing. Archiv., Vol. 17, No. 4, pp. 288-289, 1949. Translated as N.A.C.A. Technical Memorandum 1285, 1958.

(24) Streeter, V. L., "Handbook of Fluid Dynamics," McGraw-Hill Book Company, New York, 1961.

(25) Enger, P. F., "Tractive Force Fluctuations Around an Open Channel Perimeter as Determined From Point Velocity Measurements," a paper presented at the A.S.C.E. Convention, Phoenix, Arizona, April, 1961.